EurJOC European Journal of Organic Chemistry

FULL PAPER

DOI: 10.1002/ejoc.201403415

Solvent-Induced Reversal of Enantioselectivity in the Synthesis of Succinimides by the Addition of Aldehydes to Maleimides Catalysed by Carbamate-Monoprotected 1,2-Diamines

Jesús Flores-Ferrándiz,[a] Béla Fiser,[b] Enrique Gómez-Bengoa,[b] and Rafael Chinchilla*[a]

Keywords: Asymmetric catalysis / Organocatalysis / Michael addition / Enantioselectivity / Solvent effects / Transition states

A simple change in the polarity of the solvent allows both enantiomers of substituted succinimides to be obtained in the enantioselective conjugate addition reaction of aldehydes, mainly α,α-disubstituted, to maleimides catalysed by chiral carbamate-monoprotected *trans*-cyclohexane-1,2-diamines. Using a single enantiomer of the organocatalyst, both enantiomers of the resulting Michael adducts are obtained in high yields by simply changing the reaction solvent from aqueous DMF (up to 84 % *ee*) to chloroform (up to 86 % *ee*). Theoretical calculations are used to explain this uncommon reversal of the enantioselectivity; two transition state orientations of different polarities are differently favoured in polar or nonpolar solvents.

Introduction

In enantioselective organocatalysis, as in any asymmetric catalysis, opposite enantiomeric products are typically obtained by using opposite enantiomers of the organocatalysts. However, being able to switch the enantioselectivity of an organocatalytic reaction simply by changing the reaction conditions is an exciting matter of great potential interest. One of the main reasons for this is that having both enantiomeric forms of certain organocatalysts can be difficult or costly.

Although it is rare, there are some reported examples of enantioselective organocatalytic reactions where both enantiomers are obtained using a single enantiomer of the catalyst. These results are always unexpected and serendipitous.[1] Thus, a few examples of switching the enantioselectivity of an organocatalytic process by changing the counteranion in the catalyst,[2] by adding bases,[3] acids,[4] or other additives,[5] or even by light irradiation[6] have been reported.

However, it would be simpler just to change the reaction solvent, and some examples of solvent-dependent enantioselectivity reversal have been reported. Thus, an inversion of enantioselectivity was discovered in the enantioselective Michael addition of dimethyl malonate to chalcone catalysed by a quininium ammonium salt when the reaction medium was changed from conventional organic solvents to ionic liquids.[7] A solvent-dependent enantioselectivity reversal was also observed when the imidazolidinone salt **1** was used as an organocatalyst in the Michael addition of an indole to acrolein for the synthesis of a pyrroloindoline.[8] Later, α,α-phenylprolinol silyl ether **2** was shown to catalyse the enantioselective α-phenylselenenylation of isovaleraldehyde, and a change in the sense of the enantioselectivity was observed when the polarity of the solvent was changed.[9] A similar solvent-influenced reversal of the enantioselectivity of this α-phenylselenenylation reaction was also reported when polystyrene-supported imidazolidinone **3** was used as a recoverable organocatalyst.[10]

An inversion of enantioselectivity induced by a change in the solvent has also been observed in the enantioselective Michael addition of cyclohexanone to chalcones using 1-ethyl-3-methylimidazolium-(*S*)-2-pyrrolidinecarboxylic acid salt as an organocatalyst.[11] Furthermore, some conformationally flexible organocatalysts have been used in reactions in which the sense of enantioselectivity is solvent dependent: peptidic system **4** in the aldol reaction between cyclohexanone and *p*-nitrobenzaldehyde,[12] and bisthiourea/guanidine **5** in a recent Mannich-type addition of malonates to *N*-Boc-protected (Boc = *tert*-butoxycarbonyl) aldimines.[13] No explanation for why a particular enantiomer of the final product is obtained using one solvent and the opposite enantiomer is obtained using another has been given in any of the reported cases.

[a] Departamento de Química Orgánica, Facultad de Ciencias, and Instituto de Síntesis Orgánica (ISO), Universidad de Alicante, Apdo. 99, 03080 Alicante, Spain
E-mail: chinchilla@ua.es
http://dqorg.ua.es/en/
[b] Departamento de Química Orgánica I, Universidad del País Vasco,
Apdo. 1072, 20080 San Sebastián, Spain

Supporting information for this article is available on the WWW under http://dx.doi.org/10.1002/ejoc.201403415.

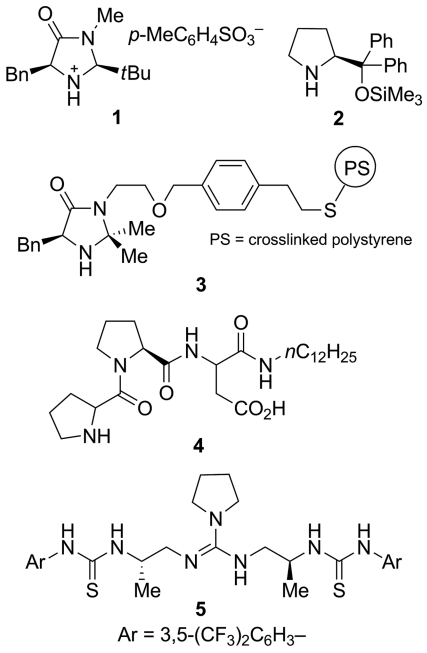

1 2 3 4 5

From the huge array of enantioselective organocatalytic reactions, those leading to enantioenriched substituted succinimides have aroused interest in recent years. These compounds are present in natural products and some clinical drug candidates,[14] and can be transformed into γ-lactams,[15] which are subunits for the design of pharmaceutical agents important in the treatment of cancer,[16] epilepsy,[17] HIV,[18] neurodegenerative disease, and depression.[19]

The easiest and most direct way of preparing enantioenriched succinimide moieties is by organocatalytic enantioselective Michael addition of carbon nucleophiles to maleimides.[20] These carbon nucleophiles can be generated by α-deprotonation of pro-nucleophiles using chiral bifunctional organocatalysts bearing both a basic tertiary amine and an acidic moiety able to coordinate the maleimide.[20] However, when aldehydes are used as pro-nucleophiles, tertiary amines are not basic enough to generate an enolate, and the enantioselective Michael addition reaction is carried out by using amine-contaning organocatalysts that can form a transient enamine with the reacting aldehyde.[21]

The first organocatalytic Michael addition of aliphatic aldehydes to *N*-aryl-substituted maleimides used α,α-phenylprolinol silyl ether as an organocatalyst, but the "difficult" α,α-disubstituted aldehydes resulted in much lower enantioselectivities.[22] Since then, different chiral bifunctional primary-amine-containing organocatalysts have been applied to the enantioselective Michael addition of these α,α-disubstituted aldehydes to maleimides leading to enantioenriched succinimides. Most of the catalysts were primary amine thioureas,[23] but primary amine guanidines,[24] amino acids,[25] amino acids combined with amine thioureas,[26] amines,[27] and 1,2-diamines[28] have also been used.

In this paper, we describe how a simple change of the reaction solvent can produce a reversal of the enantioselectivity of the conjugate addition of aldehydes to maleimides catalysed by chiral carbamate-monoprotected *trans*-cyclohexane-1,2-diamines.[29] In this way, a single enantiomeric form of a simple organocatalyst can be used for the preparation of both enantiomeric forms of the corresponding substituted succinimides. The origin of this uncommon solvent-dependent enantioswitching can be explained by theoretical calculations.

Results and Discussion

We attempted to explore the behaviour of chiral mono-Boc-protected diamine **6** as a primary-amine-containing bifunctional organocatalyst for the enantioselective conjugate addition reaction of aldehydes to *N*-substituted maleimides. This Boc-containing amine **6** was obtained following a reported procedure involving the reaction of (1*S*,2*S*)-cyclohexane-1,2-diamine with 1 equiv. of hydrogen chloride, followed by treatment with di-*tert*-butyl carbonate.[30] The enantioselective Michael addition of isobutyraldehyde to *N*-phenylmaleimide was chosen as a model reaction to test the efficiency of **6** as an organocatalyst (Table 1).

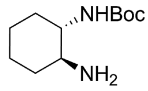

6

Initially, primary amine **6** (20 mol-%) was used in toluene as solvent at room temperature, and this gave succinimide (*S*)-**9aa** almost quantitatively with 67% *ee* (Table 1, entry 1). The absolute configuration for **9aa** was determined according to the order of elution of the corresponding enantiomers in chiral HPLC (see Exp. Section).[24b] When hexane was used as solvent, the enantioselectivity for (*S*)-**9aa** increased to 73% *ee*, whereas the use of ethyl ether resulted in a lower *ee* (Table 1, entries 2 and 3). When CH_2Cl_2 and $CHCl_3$ were used as solvents, 63 and 75% *ee* values, respectively, for (*S*)-**9aa** were observed (Table 1, entries 4 and 5).

Unexpectedly, when DMF was used as solvent, the enantioselectivity of the process reversed totally, and the oppositely configured succinimide [i.e., (*R*)-**9aa**]was obtained in high yield and with 62% *ee*, albeit with a much lower reaction rate (Table 1, entry 6). The use of solvents such as 1,4-dioxane or acetone also gave (*R*)-**9aa** with lower *ee* values (Table 1, entries 7 and 8). When water was used as the solvent, the rate of the reaction increased considerably and (*R*)-**9aa** was formed almost quantitatively, albeit with only 32% *ee* (Table 1, entry 9). Therefore, combining the highest *ee* and reaction rate, we explored the use of mixtures of DMF and H_2O as reaction solvent. Thus, different DMF/H_2O v/v ratios were tested (Table 1, entries 10–12). A 2:1, v/v mixture of DMF and H_2O gave (*R*)-**9aa** in 90% yield with 84% *ee* (Table 1, entry 11).

Having established the most appropriate solvents for achieving a reversal in the enantioselectivity [i.e., $CHCl_3$ for (*S*)-**9aa**, and DMF/H_2O (2:1, v/v) for (*R*)-**9aa**], we decided

Table 1. Screening and optimization of the reaction conditions for the reversal of the enantioselectivity in the Michael addition reaction.

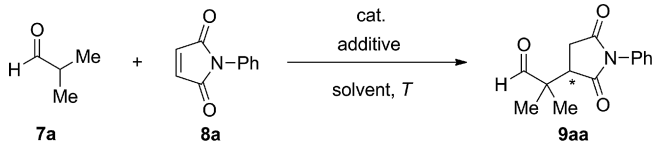

7a 8a 9aa

Entry	Catalyst (mol-%)	Additive (mol-%)[a]	Solvent	T [°C]	t [h]	Yield [%][b]	*ee* [%][c]
1	**6** (20)	–	PhMe	25	20	98	67 (*S*)
2	**6** (20)	–	hexane	25	14	85	73 (*S*)
3	**6** (20)	–	Et_2O	25	14	95	32 (*S*)
4	**6** (20)	–	CH_2Cl_2	25	20	95	63 (*S*)
5	**6** (20)	–	$CHCl_3$	25	20	99	75 (*S*)
6	**6** (20)	–	DMF	25	44	94	62 (*R*)
7	**6** (20)		dioxane	25	50	85	58 (*R*)
8	**6** (20)		acetone	25	44	92	57 (*R*)
9	**6** (20)	–	H_2O	25	2	97	32 (*R*)
10	**6** (20)	–	DMF/H_2O[d]	25	17	94	70 (*R*)
11	**6** (20)	–	DMF/H_2O[e]	25	20	90	84 (*R*)
12	**6** (20)	–	DMF/H_2O[f]	25	24	88	80 (*R*)
13	**6** (10)	–	$CHCl_3$	25	20	97	86 (*S*)
14	**6** (10)	–	DMF/H_2O[e]	25	20	95	84 (*R*)
15	**6** (5)	–	$CHCl_3$	25	40	95	76 (*S*)
16	**6** (5)	–	DMF/H_2O[e]	25	40	93	82 (*R*)
17	**6** (10)	–	$CHCl_3$	0	48	94	70 (*S*)
18	**6** (10)	–	DMF/H_2O[e]	0	48	91	82 (*R*)
19	**6** (10)	HDA (10)	$CHCl_3$	25	22	98	78 (*S*)
20	**6** (10)	HDA (10)	DMF/H_2O[e]	25	20	86	80 (*R*)
21	**6** (10)	$PhCO_2H$ (10)	$CHCl_3$	25	22	93	78 (*S*)
22	**6** (10)	$PhCO_2H$ (10)	DMF/H_2O[e]	25	22	84	80 (*R*)
23	**6** (10)	Imidazole (10)	$CHCl_3$	25	22	97	78 (*S*)
24	**6** (10)	Imidazole (10)	DMF/H_2O[e]	25	22	90	77 (*R*)
25	*ent*-**6** (10)	–	$CHCl_3$	25	20	97	84 (*R*)
26	*ent*-**6** (10)	–	DMF/H_2O[e]	25	20	94	83 (*S*)
27	**12** (10)	–	$CHCl_3$	25	24	98	81 (*S*)
28	**12** (10)	–	DMF/H_2O[e]	25	24	94	78 (*R*)
29	**13** (10)	–	$CHCl_3$	25	48	97	86 (*S*)
30	**13** (10)	–	DMF/H_2O[e]	25	48	96	78 (*R*)

[a] HDA: hexanedioic acid. [b] Isolated yield after flash chromatography. [c] Enantioselectivities and absolute stereochemistry determined by chiral HPLC[24b] analysis of the crude product mixture. [d] 1:1, v/v. [e] 2:1, v/v. [f] 4:1, v/v.

to lower the organocatalyst loading. Thus, both solvents were used with 10 and 5 mol-% organocatalyst loadings (Table 1, entries 13–16), and higher enantioselectivities for both the *S* and *R* stereoisomers were observed when a loading of 10 mol-% of **6** was used [86% *ee* for (*S*)-**9aa**, and 84% *ee* for (*R*)-**9aa**] (Table 1, entries 13 and 14). Lowering the reaction temperature to 0 °C resulted in a diminished enantioselectivity for **9aa** (Table 1, entries 17 and 18).

We then explored the influence of the presence of additives, using an optimized 10 mol-% loading of organocatalyst **6**, and $CHCl_3$ and DMF/H_2O (2:1, v/v) as enantioswitching solvents. Thus, hexanedioic (HDA) or benzoic acids were used as additives (10 mol-%), but no increase in the enantioselectivity was observed for either enantiomer (Table 1, entries 19–22). Imidazole was also tested as an additive (10 mol-%), as its presence has been shown to be beneficial in this Michael addition reaction,[24b] but lower enantioselectivities for both enantiomers of **9aa** were also observed here (Table 1, entries 23 and 24).

Attempting to achieve opposite enantioselectivities to those obtained using organocatalyst **6**, we obtained its enantiomer *ent*-**6**, following an identical procedure but starting from (1*R*,2*R*)-cyclohexane-1,2-diamine. Using this mono-Boc-protected diamine *ent*-**6** as organocatalyst, under the most convenient reaction conditions [i.e., organocatalyst (10 mol-%), room temperature, $CHCl_3$ or DMF/H_2O (2:1, v/v) as solvent], the expected opposite enantioselectivities were observed [i.e., (*R*)-**9aa** using $CHCl_3$ as solvent, and (*S*)-**9aa** using DMF/H_2O (2:1, v/v)] (Table 1, entries 25 and 26).

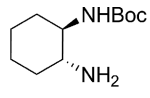

ent-**6**

We then explored the possibility of achieving this solvent-dependent reversal of enantioselectivity using chiral *trans*-cyclohexane-1,2-diamines monoprotected with other carbamates as organocatalysts. We chose the frequently used benzyloxycarbonyl (Cbz) and fluorenylmethoxycarbonyl (Fmoc) protecting groups. Thus, Cbz- and Fmoc-

monoprotected diamines **12** and **13**, respectively, were prepared by reaction of *N*-Boc-monoprotected diamine **6** with the corresponding chloroformates to give diprotected compounds **10** and **11**, followed by trifluoroacetic acid (TFA)-induced *N*-Boc deprotection (Scheme 1).

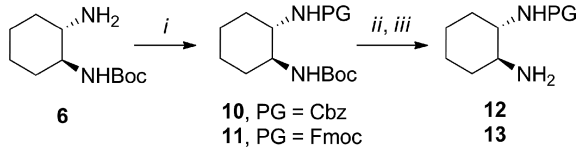

Scheme 1. (i) CbzCl (for **10**) or FmocCl (for **11**), $NaHCO_3$ (aq.), dioxane, room temp.; (ii) TFA, CH_2Cl_2, r.t.; (iii) NH_4OH, CH_2Cl_2, r.t.

These Cbz- and Fmoc-monoprotected chiral diamines **12** and **13**, respectively, were also tested as organocatalysts in the model Michael addition reaction, using the most convenient reaction conditions as determined above [i.e., organocatalyst (10 mol-%), room temperature, $CHCl_3$ or DMF/H_2O (2:1, v/v) as solvent] (Table 1, entries 27–30). Again, a reversal in the enantioselectivity of the process was observed when changing the solvent between $CHCl_3$ (*S* enantiomer) and DMF/H_2O (2:1, v/v) (*R* enantiomer). Thus, when mono-Cbz-protected diamine **12** was used as organocatalyst, *ee* values of 81% *ee* for (*S*)-**9aa** and 78% *ee* for (*R*)-**9aa** were obtained (Table 1, entries 27 and 28). When Fmoc-containing primary amine **13** was used as the organocatalyst, it gave a similar enantioselectivity for (*S*)-**9aa** to when Boc derivative **6** was used, but after a much longer reaction time, whereas the enantioselectivity for (*R*)-**9aa** was lower (Table 1, entries 29 and 30).

Once the most effective organocatalyst and reaction conditions [i.e., **6** (10 mol-%), $CHCl_3$ for the *S* enantiomer, and DMF/H_2O (2:1, v/v) for the *R* enantiomer, room temp.] were established, we went on to explore the extension of this organocatalytic solvent-dependent method to other aldehydes and maleimides (Table 2). As for the model reaction, the absolute configurations of the known succinimide products were assigned according to the order of elution of their enantiomers in chiral HPLC when compared to the literature (see Experimental section).

Table 2. Solvent-dependent reversal of enantioselectivity in the Michael addition of aldehydes to maleimides catalysed by *N*-Boc-monoprotected 1,2-diamine **6**.

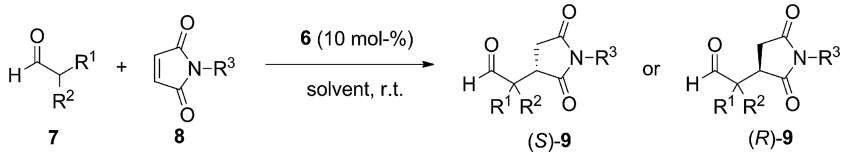

Entry	Aldehyde R¹	R²	7	Maleimide R³	8	Solvent	*t* [h]	Succinimide	Yield [%][a]	*ee* [%][b,c]
1	Me	Me	**7a**	Ph	**8a**	$CHCl_3$	20	(*S*)-**9aa**	97	86
2						DMF/H_2O, 2:1	20	(*R*)-**9aa**	95	84
3	Me	Me	**7a**	3-ClC_6H_4	**8b**	$CHCl_3$	30	(*S*)-**9ab**	99	38
4						DMF/H_2O, 2:1	30	(*R*)-**9ab**	96	76
5	Me	Me	**7a**	4-ClC_6H_4	**8c**	$CHCl_3$	30	(*S*)-**9ac**	99	60
6						DMF/H_2O, 2:1	30	(*R*)-**9ac**	97	74
7	Me	Me	**7a**	4-BrC_6H_4	**8d**	$CHCl_3$	30	(*S*)-**9ad**	99	70
8						DMF/H_2O, 2:1	30	(*R*)-**9ad**	98	70
9	Me	Me	**7a**	4-AcC_6H_4	**8e**	$CHCl_3$	26	(*S*)-**9ae**	92	40
10						DMF/H_2O, 2:1	26	(*R*)-**9ae**	15	80
11	Me	Me	**7a**	2-$MeOC_6H_4$	**8f**	$CHCl_3$	32	(*S*)-**9af**	90	76
12						DMF/H_2O, 2:1	32	(*R*)-**9af**	92	74
13	Me	Me	**7a**	Bn	**8g**	$CHCl_3$	22	(*S*)-**9ag**	93	30
14						DMF/H_2O, 2:1	22	(*R*)-**9ag**	90	72
15	Me	Me	**7a**	Me	**8h**	$CHCl_3$	21	(*S*)-**9ah**	94	53
16						DMF/H_2O, 2:1	21	(*R*)-**9ah**	91	68
17	Me	Me	**7a**	H	**8i**	$CHCl_3$	17	(*S*)-**9ai**	94	50
18						DMF/H_2O, 2:1	17	(*R*)-**9ai**	88	70
19	Et	Et	**7b**	Ph	**8a**	$CHCl_3$	48	(*S*)-**9ba**	70	55
20						DMF/H_2O, 2:1	48	(*R*)-**9ba**	93	68
21	–$(CH_2)_4$–		**7c**	Ph	**8a**	$CHCl_3$	30	(*S*)-**9ca**	99	49
22						DMF/H_2O, 2:1	30	(*R*)-**9ca**	96	61
23	–$(CH_2)_5$–		**7d**	Ph	**8a**	$CHCl_3$	48	(*S*)-**9da**	96	14
24						DMF/H_2O, 2:1	48	(*R*)-**9da**	96	35
25	H	Me	**7e**	Ph	**8a**	$CHCl_3$	23	(*S,S*)/(*R,S*)-**9ea**	95[d]	36/28
26						DMF/H_2O, 2:1	23	(*R,R*)/(*S,R*)-**9ea**	96[e]	76/73

[a] Isolated yield after flash chromatography. [b] Enantioselectivities determined by chiral HPLC analysis of the crude product mixture. [c] Absolute configuration assigned by the order of elution of the enantiomers in chiral HPLC (see Experimental section). [d] Mixture of diastereomers 1.4:1, as determined by ^1H NMR (300 MHz) spectroscopic analysis of the crude product mixture. [e] Mixture of diastereomers 1.2:1, as determined by ^1H NMR (300 MHz) spectroscopic analysis of the crude product mixture.

Thus, when $CHCl_3$ was used as solvent, isobutyraldehyde reacted with *N*-phenylmaleimides bearing halogens on the phenyl ring, such as a chloro substituent at the 3- or 4-position (i.e., **8b** and **8c**, respectively), or a bromo substituent at the 4-position (i.e., **8d**), and the corresponding succinimides [i.e., (*S*)-**9ab**, (*S*)-**9ac**, and (*S*)-**9ad**] were obtained with 38, 60, and 70% *ee*, respectively (Table 2, entries 3, 5, and 7). However, when DMF/H_2O (2:1, v/v) was used as the reaction solvent, adducts (*R*)-**9ab**, (*R*)-**9ac**, and (*R*)-**9ad** were isolated with 76, 74, and 70% *ee* (Table 2, entries 4, 6, and 8). In addition, when an acetyl or a methoxy group was present on the phenyl ring of the maleimide, as in the case of **8e** and **8f**, the *ee* values the corresponding enantiomeric succinimides (*S*)-**9ae**/(*R*)-**9ae** and (*S*)-**9af**/(*R*)-**9af** were 40/80% *ee* and 76/74% *ee*, respectively, depending on whether $CHCl_3$ or DMF/H_2O (2:1, v/v) was used as the solvent (Table 2, entries 9–12).

Non-*N*-arylated maleimides were also used for the conjugate addition with isobutyraldehyde. Thus, *N*-benzylmaleimide (**8g**) gave enantiomeric succinimides (*S*)-**9ag** and (*R*)-**9ag** in high yields and with 30 and 72% *ee*, depending on the solvent used (Table 2, entries 13 and 14). Similarly, *N*-methylmaleimide (**8h**) gave the *S* and *R* enantiomers of adduct **9ah** when $CHCl_3$ and DMF/H_2O (2:1, v/v) were used as the reaction solvent (53 and 68% *ee*, respectively; Table 2, entries 15 and 16). In addition, the simple maleimide (**8i**) was also used as a Michael acceptor, and gave (*S*)-**9ai** (50% *ee*) when $CHCl_3$ was used as solvent, and (*R*)-**9ai** (70% *ee*) when the solvent was DMF/H_2O (2:1, v/v) (Table 2, entries 17 and 18).

Other α,α-disubstituted aldehydes were used for this enantioswitching organocatalytic Michael addition reaction to *N*-phenylmaleimide. Thus, 2-ethylbutanal (**7b**) gave succinimides (*S*)-**9ba** (55% *ee*) and (*R*)-**9ba** (68% *ee*) using $CHCl_3$ and DMF/H_2O (2:1, v/v) as solvents, respectively (Table 2, entries 19 and 20). In addition, cyclopentanecarbaldehyde (**7c**) and cyclohexanecarbaldehyde (**7d**) gave almost quantitative amounts of succinimides (*S*)-**9ca** and (*S*)-**9da** with 49 and 14% *ee*, respectively, when $CHCl_3$ was the reaction solvent, whereas (*R*)-**9ca** and (*R*)-**9da** were isolated with 61 and 35% *ee*, respectively, when DMF/H_2O (2:1, v/v) was used as solvent (Table 2, entries 21–24). Moreover, the use of propanal (**7e**), an α-monosubstituted aldehyde, in the two solvents allowed Michael adducts (*R*,*S*)/(*S*,*S*)-**9ea** and (*S*,*R*)/(*R*,*R*)-**9ea**, respectively, to be obtained as mixtures of diastereomers, with *ee* values of up to 36 and 76% *ee*, respectively, for the major isomer (Table 2, entries 25 and 26, see footnotes[d,e]).

In an attempt to rule out the possibility that the change in the enantioselectivity could be a consequence of a further transformation of the initially formed product, succinimide (*R*)-**9aa** obtained with 84% *ee* (Table 2, entry 2) was stirred in the presence of organocatalyst **6** (10 mol-%), in $CHCl_3$ as solvent at room temperature. After 20 h, succinimide (*R*)-**9aa** was recovered unchanged. In addition, the model reaction of aldehyde **7a** with maleimide **8a** in the presence of organocatalyst **6** (10 mol-%) in DMF/H_2O (2:1, v/v) was carried out for 4, 8, and 12 h, and the *ee* for (*R*)-**9aa** remained at 84% *ee*.

To get further insight into the origin of this solvent-dependent enantioselectivity reversal, we carried out theoretical calculations on the reaction of *N*-phenylmaleimide (**8a**) and isobutyraldehyde (**7a**) in the presence of primary-amine catalyst **6**. Different computational conditions were envisioned (see Exp. Section) − in the gas phase, in implicit solvents (water and chloroform), and also in the presence of a discrete number of explicit water molecules − in an attempt to reproduce the experimental conditions as closely as possible, since the results are highly dependent on the reaction medium. Preliminary studies showed that, as expected, the initial formation of an enamine between the catalyst and the aldehyde is followed by nucleophilic attack on the maleimide, according to Seebach's synclinal model (*endo* attack, Figure 1).[31] A key feature of this model is that the reacting face of the enamine completely diastereoselectivelyattacks only one of the faces of the maleimide. Thus, the lower face of the enamine (from our point of view in Figure 1) reacts with the *Re* face of the maleimide, and the upper face of the enamine must react with the *Si* face of the maleimide. This means that each face of the enamine produces only one of the final enantiomeric products. This fact is crucial to understanding the following discussion, which can be based solely on the reacting face of the enamine. Meanwhile, the *exo* approaches, like the one involving the lower face of the enamine and the *Si* face of the maleimide (Figure 1), are much higher in energy, and can be safely disregarded.

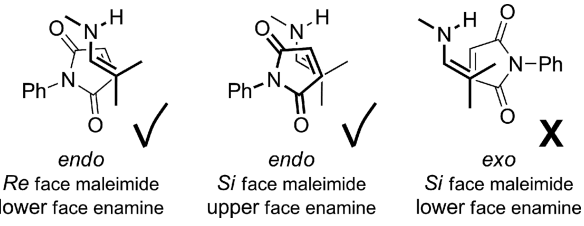

Figure 1. Faces of enamine and maleimide reacting through Seebach's synclinal model.

The initial optimizations of the enamine structures showed that in the most stable conformations (i.e., **A** and **B**, Figure 2), the NHBoc and enamine groups are in equatorial positions of the cyclohexane ring. In both cases, the NH moiety of the NHBoc carbamate is pointing *down* from our view. The two conformations differ in the orientations that the NH enamine group can present, pointing *up* (conformation **A**) or *down* (conformation **B**) from the plane of the cyclohexane ring (Figure 2). According to this picture, the fragment NH–C–C–NH shows the two NH groups in *anti* (**A**) or *syn* (**B**) relative orientations. The optimization of these structures showed that they are very similar in energy, and both must be taken into account for the transition-structure search. In fact, structure **B** is slightly more stable than **A** in $CHCl_3$ (1.0 kcal/mol difference), whereas they have the same energy in water. This means that **A** is slightly better solvated by water than by chloroform. We cautiously took these data as a first indication of the solvent dependence of the conformational distribution of the initial struc-

tures. We thought that this effect could be more dramatic during the transition states of the reaction, which are supposed to be quite polar, due to the significant charge transfer that takes place from the enamine to the maleimide.

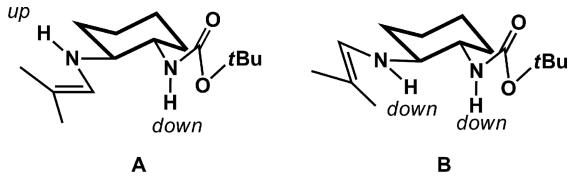

Figure 2. Most stable conformations of the reacting enamine.

We confirmed this hypothesis in the light of the computed transition state activation energies. In conformation **A**, the maleimide could hypothetically approach the two faces of the enamine, as shown in Figure 3. If the attack takes place from the left-hand side of the enamine, the reaction occurs through TS-$\mathbf{A}_{\boldsymbol{R}}$ (*Si* face of maleimide, *R* product), whereas the approach of the maleimide from the right-hand side of the enamine (hypothetical TS-$\mathbf{A}_{\boldsymbol{S}}$) is strongly disfavoured due to steric repulsion from the large Boc group, which is blocking that face. We could not actually find any transition state for that approach without severely distorting the structure. It is noteworthy that TS-$\mathbf{A}_{\boldsymbol{R}}$ is a very polar structure, with a high degree of negative charge developing in the maleimide oxygen atom. Consequently, the polarity of the reaction medium must have a great influence on the activation barrier of the process. Thus, it was not surprising to find that the lowest free energy for TS-$\mathbf{A}_{\boldsymbol{R}}$ corresponds to the structure computed in a water model ($\Delta G^{\ddagger}$ = 14.8 kcal/mol),[32] while the chloroform and gas phase models present higher values ($\Delta G^{\ddagger}$ = 18.7 and 20.7 kcal/mol, respectively). Interestingly, TS-$\mathbf{A}_{\boldsymbol{R}}$ leads to the formation of the *R* enantiomer, which is experimentally obtained in the polar aqueous medium.

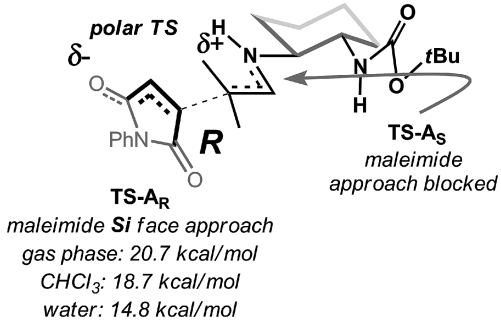

Figure 3. Computed activation energies for transition state TS-$\mathbf{A}_{\boldsymbol{R}}$ (corresponding to conformation **A** in Figure 2) in the gas phase, chloroform, and water models. Structures and values were obtained at the M06-2X/6-311+G**//M06-2X/6-31G** level of theory.

On the other hand, two transition states were located for conformation **B**, following the two possible approaching trajectories (TS-$\mathbf{B}_{\boldsymbol{S}}$ and TS-$\mathbf{B}_{\boldsymbol{R}}$, Figure 4). In TS-$\mathbf{B}_{\boldsymbol{S}}$, the *Re* face of the maleimide is attacked by the lower face (from our view) of the enamine, whereas in TS-$\mathbf{B}_{\boldsymbol{R}}$, the *Si* face of the maleimide approaches the upper face of the enamine. In TS-$\mathbf{B}_{\boldsymbol{S}}$, the maleimide oxygen and the HNBoc group are close enough to form an intermolecular hydrogen bond, which stabilizes the developing negative charge in the maleimide oxygen atom, producing a structure that is much less polar than TS-$\mathbf{A}_{\boldsymbol{R}}$, and therefore, less sensitive to the surrounding solvent molecules. This effect can be observed in the computed energies for TS-$\mathbf{B}_{\boldsymbol{S}}$, which do not show significant differences between the different solvent models, or even the gas phase (TS-$\mathbf{B}_{\boldsymbol{S}}$ *water*: 17.7,[32] TS-$\mathbf{B}_{\boldsymbol{S}}$ *chloroform*: 16.0, TS-$\mathbf{B}_{\boldsymbol{S}}$ *gas phase*: 15.8 kcal/mol, Figure 4).

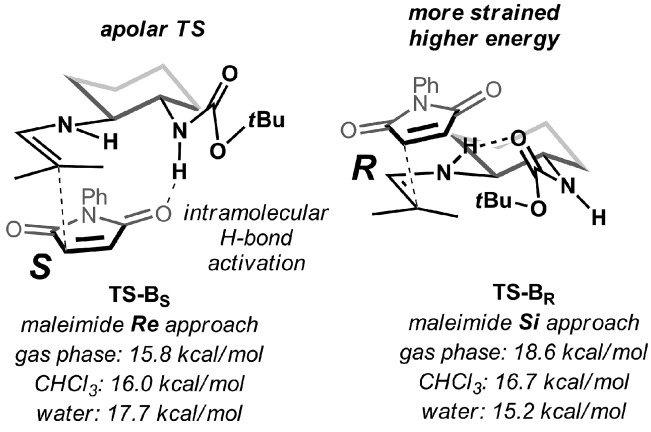

Figure 4. Representations and energies of transition states TS-$\mathbf{B}_{\boldsymbol{S}}$ and TS-$\mathbf{B}_{\boldsymbol{R}}$, corresponding to conformation **B** in Figure 2. Structures and values were obtained at the M06-2X/6-311+G**//M06-2X/6-31G** level of theory.

Meanwhile, if the maleimide approaches the upper face of the enamine in conformation B, this leads to transition state TS-$\mathbf{B}_{\boldsymbol{R}}$ (Figure 4). Similarly to TS-$\mathbf{A}_{\boldsymbol{R}}$, this transition structure is quite polar, and the maleimide oxygen is better stabilized in the presence of surrounding solvent molecules. Thus, its lowest energy was measured in water (15.2 kcal/mol),[32] although this value is higher than the one corresponding to TS-$\mathbf{A}_{\boldsymbol{R}}$ (14.8 kcal/mol, Figure 3). This increase in the energy is probably due to the higher internal strain that the structure presents as the result of a weak hydrogen bond formed between the enamine NH and the carbamate oxygen atom, which does not participate in the activation of the maleimide.

In summary, the most significant computational data are that the lowest calculated activation energy in water corresponds to TS-$\mathbf{A}_{\boldsymbol{R}}$ (14.8 kcal/mol), a polar structure lacking intramolecular hydrogen bonds, where the surrounding water molecules are responsible for intermolecular hydrogen-bonding activation of the maleimide (Figure 5). TS-$\mathbf{A}_{\boldsymbol{R}}$ produces the *R* enantiomer of the product, which is consistent with the experimental results in the polar aqueous DMF medium (Table 1). Also, the lowest calculated activation energy in chloroform is TS-$\mathbf{B}_{\boldsymbol{S}}$ (16.0 kcal/mol), a transition structure containing an intramolecular hydrogen bond between the maleimide and the NHBoc groups (Figure 5). This transition state leads to the formation of the *S* enantiomer, which is once again consistent with the experimental data in chloroform (Table 1). Furthermore, these results agree with chemical common sense, that intramolec-

ular hydrogen bonds are more significant in nonpolar solvents, whereas intermolecular hydrogen bonds with surrounding water molecules are present in aqueous systems.

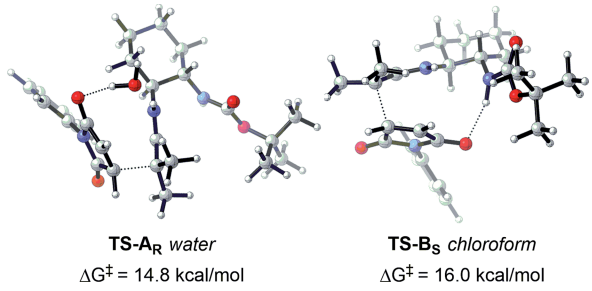

Figure 5. 3D representations and energies of transition states TS-$\mathbf{A}_R$-*water* and TS-$\mathbf{B}_S$-*chloroform*.

Conclusions

Easily prepared carbamate-monoprotected chiral *trans*-cyclohexane-1,2-diamines can be used as organocatalysts in the high-yielding enantioselective conjugate addition of aldehydes, mainly α,α-disubstituted, to different maleimides, in a solvent-dependent enantioswitchable reaction. Thus, both *S*- or *R*-enantioenriched forms of the corresponding succinimides can be obtained using a single enantiomer of the organocatalyst, just by changing the reaction solvent from chloroform to aqueous *N*,*N*-dimethylformamide. Theoretical calculations are able to show the reason for this solvent-dependent reversal of enantioselectivity. The most polar transition state (i.e., TS-$\mathbf{A}_R$) presents the lowest energy in water, and it is responsible for the major formation of the *R* enantiomer. The least polar transition state (i.e., TS-$\mathbf{B}_S$) accounts for the formation of the *S* enantiomer in chloroform, consistent with the experimental results.

Experimental Section

General Remarks: The syntheses of all organocatalysts, as well as their physical and spectroscopic data, are described in the Supporting Information. The absolute configurations of adducts **9** were determined according to the described order of elution of their enantiomers in chiral HPLC. Reference racemic samples of adducts **9** were obtained by performing the reaction using 4-methylbenzylamine (20 mol-%) as organocatalyst in toluene as solvent at 25 °C.

Typical Procedure for the Enantioselective Michael Addition Reaction: Aldehyde **7** (0.4 mmol) was added to a solution of **6** (0.04 mmol) and **8** (0.2 mmol) in $CHCl_3$ or DMF/H_2O (2:1, v/v; 0.5 mL), and the reaction was stirred at room temp. until TLC showed that it was complete. HCl (2 M aq.; 10 mL) was added, and the mixture was extracted with EtOAc (3× 10 mL). The organic phase was washed with water (2× 10 mL), dried ($MgSO_4$), filtered, and evaporated (15 Torr). The resulting residue was purified by flash chromatography (hexane/EtOAc) to give adducts **9**.

Succinimides **9** have already been described.[24b] Their ^1H and ^{13}C NMR spectroscopic data and retention times in chiral HPLC for both enantiomers can be found in the Supporting Information.

Computational Methods: The structures were initially optimized using density functional theory (DFT) with the B3LYP[33] and the 6-31G* basis set, as implemented in Gaussian 09.[34] Further reoptimization at the M06-2X/6-31G** level of theory[35] was carried out to account for the important dispersion forces in such large systems. The energy values shown in Figures 3 and 4 also include single-point refinements at the M06-2X/6-311+G** level on the previously optimized structures (M06-2X/6-31G**), including polarization functions for a better description of hydrogen-bond activations. Additionally, solvation factors were introduced with the IEF-PCM method,[36] using chloroform or water as indicated in the text and figures.

We also performed single-point calculations at the B3LYP/6-311+G** level of theory, and the relative values are similar to those of the M06-2X energies. Therefore, they have not been included in the manuscript, and are collected in the Supporting Information. The stationary points were characterized by frequency calculations in order to verify that they have the right number of imaginary frequencies.

The intrinsic reaction coordinates (IRC)[37] were followed to verify the energy profiles connecting each transition state to the correct associated local minima.

Acknowledgments

The authors are grateful for the financial support from the Spanish Ministerio de Economía y Competitividad (MEC) (project number CTQ2011-24151), Fondos Europeos para el Desarrollo Regional (FEDER), the COST Action CM0905 "Organocatalysis", the FP7 Marie Curie Action of the European Commission via the ITN ECHONET Network (FP7-MCITN-2012-316379), the University of Alicante and the University of the Basque Country. The authors also thank SGI/IZO-SGIker (UPV/EHU) and the University of Szeged, Department of Chemical Informatics for allocation of computational resources. J. F.-F. acknowledges the Vicerrectorado de Investigación, Desarrollo e Innovación of the University of Alicante for a predoctoral fellowship.

[1] M. Bartók, *Chem. Rev.* **2010**, *110*, 1663–1705.
[2] P. Mazón, R. Chinchilla, C. Nájera, G. Guillena, R. Kreiter, R. J. M. Klein Gebbink, G. van Koten, *Tetrahedron: Asymmetry* **2002**, *13*, 2181–2185.
[3] a) S.-H. Chen, B.-C. Hong, C.-F. Su, S. Sarshar, *Tetrahedron Lett.* **2005**, *46*, 8899–8903; b) D. G. Blackmond, A. Moran, M. Hughes, A. Armstrong, *J. Am. Chem. Soc.* **2010**, *132*, 7598–7599.
[4] S. A. Moteki, J. Han, S. Arimitsu, M. Akakura, K. Nakayama, K. Maruoka, *Angew. Chem. Int. Ed.* **2012**, *51*, 1187–1190; *Angew. Chem.* **2012**, *124*, 1213–1216.
[5] a) S. Arseniyadis, P. V. Subhash, A. Valleix, S. P. Mathew, D. G. Blackmond, A. Wagner, C. Mioskowski, *J. Am. Chem. Soc.* **2005**, *127*, 6138–6139; b) F.-C. Wu, C.-S. Da, Z.-X. Du, Q.-P. Guo, W.-P. Li, L. Yi, Y.-N. Jia, X. Ma, *J. Org. Chem.* **2009**, *74*, 4812–4818.
[6] J. Wang, B. L. Feringa, *Science* **2011**, *331*, 1429–1432.
[7] R. T. Dere, R. R. Pal, P. S. Patil, M. M. Salunkhe, *Tetrahedron Lett.* **2003**, *44*, 5351–5353.
[8] J. F. Austin, S.-G. Kim, C. J. Sinz, W.-J. Xiao, D. W. C. MacMillan, *Proc. Natl. Acad. Sci. USA* **2004**, *101*, 5482–5487.
[9] H. Sunden, R. Rios, A. Cordova, *Tetrahedron Lett.* **2007**, *48*, 7865–7869.
[10] F. Giacalone, M. Gruttadauria, P. Agrigento, V. Campisciano, R. Noto, *Catal. Commun.* **2011**, *16*, 75–80.
[11] Y. Qian, S. Xiao, L. Liu, Y. Wang, *Tetrahedron: Asymmetry* **2008**, *19*, 1515–1518.

[12] M. Messerer, H. Wennemers, *Synlett* **2011**, 499–502.
[13] a) Y. Sohtome, T. Yamaguchi, S. Tanaka, K. Nagasawa, *Org. Biomol. Chem.* **2013**, *11*, 2780–2786; b) Y. Sohtome, K. Nagasawa, *Org. Biomol. Chem.* **2014**, *12*, 1681–1685.
[14] a) A. Fredenhagen, S. Y. Tamura, P. T. M. Kenny, H. Komura, Y. Naya, K. Nakanishi, K. Nishiyama, M. Sugiura, H. Kita, *J. Am. Chem. Soc.* **1987**, *109*, 4409–4411; b) C. Malochet-Grivois, C. Roussakis, N. Robillard, J. F. Biard, D. Riou, C. Debitus, J. F. Verbist, *Anti-Cancer Drug Des.* **1992**, *7*, 493–502; c) Y. Ando, E. Fuse, W. D. Figg, *Clin. Cancer Res.* **2002**, *8*, 1964–1973; d) C. Freiberg, N. A. Brunner, G. Schiffer, T. Lampe, J. Pohlmann, M. Brands, M. Raabe, D. Haebich, K. Ziegelbauer, *J. Biol. Chem.* **2004**, *279*, 26066–26073; e) M. Isaka, N. Rugseree, P. Maithip, P. Kongsaeree, S. Prabpai, Y. Thebtaranonth, *Tetrahedron* **2005**, *61*, 5577–5583; f) J. Uddin, K. Ueda, E. R. O. Siwu, M. Kita, D. Uemura, *Bioorg. Med. Chem.* **2006**, *14*, 6954–6961; g) M. N. Aboul-Enein, A. A. El-Azzouny, O. A. Saleh, Y. A. Maklad, *Mini-Rev. Med. Chem.* **2012**, *12*, 671–700.
[15] a) J. Nöth, K. J. Frankowski, B. Neuenswander, J. Aubé, O. Reiser, *J. Comb. Chem.* **2008**, *10*, 456–459; b) E. Fenster, D. Hill, O. Reiser, J. Aube, *Beilstein J. Org. Chem.* **2012**, *8*, 1804–1813.
[16] D. Chauhan, L. Catley, G. Li, K. Podar, T. Hideshima, M. Velankar, C. Mitsiades, N. Mitsiades, H. Yasui, A. Letai, H. Ovaa, C. Berkers, B. Nicholson, T.-H. Chao, S. T. C. Neuteboom, P. Richardson, M. A. Palladino, K. C. Anderson, *Cancer Cell* **2005**, *8*, 407–419.
[17] a) P. A. Reddy, B. C. H. Hsiang, T. N. Latifi, M. W. Hill, K. E. Woodward, S. M. Rothman, J. A. Ferrendelli, D. F. Covey, *J. Med. Chem.* **1996**, *39*, 1898–1906; b) K. Das Sarma, J. Zhang, Y. Huang, J. G. Davidson, *Eur. J. Org. Chem.* **2006**, 3730–3737.
[18] a) A. Spaltenstein, M. R. Almond, W. J. Bock, D. G. Cleary, E. S. Furfine, R. J. Hazen, W. M. Kazmierski, F. G. Salituro, R. D. Tung, L. L. Wright, *Bioorg. Med. Chem. Lett.* **2000**, *10*, 1159–1162; b) W. M. Kazmierski, W. Andrews, E. Furfine, A. Spaltenstein, L. Wright, *Bioorg. Med. Chem. Lett.* **2004**, *14*, 5689–5692.
[19] a) D. M. Barnes, J. Ji, M. G. Fickes, M. A. Fitzgerald, S. A. King, H. E. Morton, F. A. Plagge, M. Preskill, S. H. Wagaw, S. J. Wittenberger, J. Zhang, *J. Am. Chem. Soc.* **2002**, *124*, 13097–13105; b) K. Tang, J.-T. Zhang, *Neurol. Res.* **2002**, *24*, 473–478.
[20] P. Chauhan, J. Kaur, S. S. Chimni, *Chem. Asian J.* **2012**, *8*, 328–346.
[21] a) O. V. Serdyuk, C. M. Heckel, S. B. Tsogoeva, *Org. Biomol. Chem.* **2013**, *11*, 7051–7071; b) A. Desmarchelier, V. Coeffard, X. Moreau, C. Greck, *Tetrahedron* **2014**, *70*, 2491–2513.
[22] G.-L. Zhao, Y. Xu, H. Sundén, L. Eriksson, M. Sayah, A. Cordova, *Chem. Commun.* **2007**, 734–735.
[23] a) F. Yu, Z. Jin, H. Huang, T. Ye, X. Liang, J. Ye, *Org. Biomol. Chem.* **2010**, *8*, 4767–4774; b) J.-F. Bai, L. Peng, L.-l. Wang, L.-X. Wang, X.-Y. Xu, *Tetrahedron* **2010**, *66*, 8928–8932; c) F. Xue, L. Liu, S. Zhang, W. Duan, W. Wang, *Chem. Eur. J.* **2010**, *16*, 7979–7982; d) T. Miura, S. Nishida, A. Masuda, N. Tada, A. Itoh, *Tetrahedron Lett.* **2011**, *52*, 4158–4160; e) T. Miura, A. Masuda, M. Ina, K. Nakashima, S. Nishida, N. Tada, A. Itoh, *Tetrahedron: Asymmetry* **2011**, *22*, 1605–1609; f) Z.-w. Ma, Y.-x. Liu, P.-l. Li, H. Ren, Y. Zhu, J.-c. Tao, *Tetrahedron: Asymmetry* **2011**, *22*, 1740–1748; g) Z.-W. Ma, Y.-X. Liu, W.-J. Zhang, Y. Tao, Y. Zhu, J.-C. Tao, M.-S. Tang, *Eur. J. Org. Chem.* **2011**, 6747–6754; h) M. Durmaz, A. Sirit, *Tetrahedron: Asymmetry* **2013**, *24*, 1443–1448; i) S. Orlandi, G. Pozzi, M. Ghisetti, M. Benaglia, *New J. Chem.* **2013**, *37*, 4140–4147.
[24] a) A. Avila, R. Chinchilla, C. Nájera, *Tetrahedron: Asymmetry* **2012**, *23*, 1625–1627; b) A. Avila, R. Chinchilla, E. Gómez-Bengoa, C. Nájera, *Eur. J. Org. Chem.* **2013**, 5085–5092.
[25] a) T. C. Nugent, A. Sadiq, A. Bibi, T. Heine, L. L. Zeonjuk, N. Vankova, B. S. Bassil, *Chem. Eur. J.* **2012**, *18*, 4088–4098; b) C. G. Kokotos, *Org. Lett.* **2013**, *15*, 2406–2409.
[26] S. Muramulla, J.-A. Ma, J. C.-G. Zhao, *Adv. Synth. Catal.* **2013**, *355*, 1260–1264.
[27] W. Yang, K.-Z. Jiang, X. Lu, H.-M. Yang, L. Li, Y. Lu, L.-W. Xu, *Chem. Asian J.* **2013**, *8*, 1182–1190.
[28] A. Avila, R. Chinchilla, E. Gómez-Bengoa, C. Nájera, *Tetrahedron: Asymmetry* **2013**, *24*, 1531–1535.
[29] Communication: J. Flores-Ferrándiz, R. Chinchilla, *Tetrahedron: Asymmetry* **2014**, *25*, 1091–1094.
[30] D. W. Lee, H.-J. Ha, W. K. Lee, *Synth. Commun.* **2007**, *37*, 737–742.
[31] a) D. Seebach, J. Golinski, *Helv. Chim. Acta* **1981**, *64*, 1413–1423; b) D. Seebach, A. K. Beck, J. Golinski, J. N. Hay, T. Laube, *Helv. Chim. Acta* **1985**, *68*, 162–172.
[32] The energies in water shown in Figures 3 and 4 were obtained using a water model system in the presence of one explicit molecule of water. When an implicit water model was used, the calculated energies showed a similar trend: TS-$\mathbf{A}_{\boldsymbol{R}}$: 15.8 kcal/mol, TS-$\mathbf{B}_{\boldsymbol{S}}$: 16.9 kcal/mol, TS-$\mathbf{B}_{\boldsymbol{R}}$: 16.9 kcal/mol; see the Supporting Information for further details.
[33] a) C. Lee, W. Yang, R. G. Parr, *Phys. Rev. B* **1988**, *37*, 785–789; b) A. D. Becke, *J. Chem. Phys.* **1993**, *98*, 5648–5652; c) W. Kohn, A. D. Becke, R. G. Parr, *J. Phys. Chem.* **1996**, *100*, 12974–12980.
[34] M. J. Frisch, G. W. Trucks, H. B. Schlegel, G. E. Scuseria, M. A. Robb, J. R. Cheeseman, G. Scalmani, V. Barone, B. Mennucci, G. A. Petersson, H. Nakatsuji, M. Caricato, X. Li, H. P. Hratchian, A. F. Izmaylov, J. Bloino, G. Zheng, J. L. Sonnenberg, M. Hada, M. Ehara, K. Toyota, R. Fukuda, J. Hasegawa, M. Ishida, T. Nakajima, Y. Honda, O. Kitao, H. Nakai, T. Vreven, J. A. Montgomery Jr., J. E. Peralta, F. Ogliaro, M. Bearpark, J. J. Heyd, E. Brothers, K. N. Kudin, V. N. Staroverov, R. Kobayashi, J. Normand, K. Raghavachari, A. Rendell, J. C. Burant, S. S. Iyengar, J. Tomasi, M. Cossi, N. Rega, J. M. Millam, M. Klene, J. E. Knox, J. B. Cross, V. Bakken, C. Adamo, J. Jaramillo, R. Gomperts, R. E. Stratmann, O. Yazyev, A. J. Austin, R. Cammi, C. Pomelli, J. W. Ochterski, R. L. Martin, K. Morokuma, V. G. Zakrzewski, G. A. Voth, P. Salvador, J. J. Dannenberg, S. Dapprich, A. D. Daniels, O. Farkas, J. B. Foresman, J. V. Ortiz, J. Cioslowski, D. J. Fox, *Gaussian 09*, revision E.01, Gaussian, Inc., Wallingford CT, **2009**.
[35] Y. Zhao, D. G. Truhlar, *Theor. Chem. Acc.* **2008**, *120*, 215–241.
[36] a) E. Cancès, B. Mennucci, J. Tomasi, *J. Chem. Phys.* **1997**, *107*, 3032–3047; b) J. Tomasi, B. Mennucci, E. Cancès, *THEOCHEM* **1999**, *464*, 211–226.
[37] C. González, H. B. Schlegel, *J. Phys. Chem.* **1990**, *94*, 5523–5527.

Received: October 31, 2014
Published Online: ■

EurJOC European Journal of Organic Chemistry

Organocatalysis

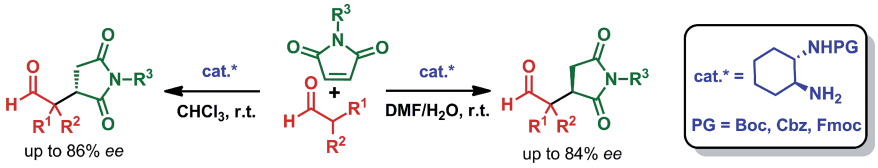

An inversion of enantioselectivity is achieved by simply changing the solvent in the enantioselective Michael addition reaction of aldehydes to maleimides catalysed by carbamate-monoprotected *trans*-cyclohexane-1,2-diamines. The reasons behind this uncommon enantioswitch are explained using theoretical calculations.

Keywords: Asymmetric catalysis / Organocatalysis / Michael addition / Enantioselectivity / Solvent effects / Transition states

